fuels

MDPI

Case Report

Thermal Activation of Digested Sewage Sludges for Carbon Dioxide Removal from Biogas

Mirko Tinnirello [1], Davide Papurello [1,2,*], Massimo Santarelli [1] and Sonia Fiorilli [3]

[1] Energy Department (DENERG), Politecnico di Torino, Corso Duca degli Abruzzi, 24, 10100 Turin, Italy; mirko.tinnirello@gmail.com (M.T.); massimo.santarelli@polito.it (M.S.)
[2] Energy Center, Politecnico di Torino, Via Paolo Borsellino 38/16, 10138 Turin, Italy
[3] Department of Applied Science and Technology (DISAT), Politecnico di Torino, Corso Duca degli Abruzzi, 24, 10100 Turin, Italy; sonia.fiorilli@polito.it
* Correspondence: davide.papurello@polito.it

Received: 21 September 2020; Accepted: 20 October 2020; Published: 22 October 2020

Abstract: Anaerobically digested sewage sludges were used as feedstock in the production of activated carbons through physical activation. These char samples were experimentally tested as adsorbents for the removal of CO_2 from a simulated biogas mixture. The CO_2 concentration level allowed in biomethane was fixed from the European Standards EN 16723-1 and EN 16723-2. The char yield and the subsequent adsorption capacity values were studied, considering the operating parameters of the process. A physical activation process was considered with the following parameters: the temperature, the dwell time, the activating agent, the heating rate, the flow rate, and the method. Among the adsorption tests, the activating temperature and the agent employed affected the CO_2 removal. The maximum adsorption capacity was achieved with nitrogen as an activating agent at 600 °C, with 2 h of dwell time (102.5 mg/g).

Keywords: pyrolysis; circular economy; wastewater; sewage sludges; biomethane; CO_2 removal

1. Introduction

The amount of sludge produced from human activities has increased greatly due to industrialization and urbanization during the past century. In Europe, the progressive implementation of the Urban Waste Water Treatment Directive 91/271/EEC in all Member States has enhanced the quantities of the sewage sludge requiring disposal, highlighting the necessity to investigate for reliable, environmentally-benign and lasting technological solutions [1]. This typology of waste can be considered as an urban burden, or as a valuable resource. This is related to the style of waste management. The concept reported above is internationally recognized as a circular approach for the recovery of matter, energy and economic value from waste [2–6]. Based on key literature studies, the Circular Economy can be defined as: a regenerative system in which resource input and waste, emission, and energy leakage are minimised by slowing, closing, and narrowing material and energy loops. This can be achieved through long-lasting design, maintenance, repair, reuse, remanufacturing, refurbishing, and recycling. Second, we define sustainability as the balanced integration of economic performance, social inclusiveness, and environmental resilience, to the benefit of current and future generations [7]. The disposal of the treated sewage sludges coming from the wastewater treatment plants (WWTP) has been traditionally accomplished by the application of this waste mainly for landfilling, soil conditioning, fertilization, the production of building materials (e.g., concrete, bituminous mixtures), and road construction, etc. [8]. Another interesting disposal solution is represented by the thermal route. Energy can be recovered using thermal processes, involving incineration, gasification or pyrolysis, or specific mild pyrolysis, also called torrefaction.

These techniques allow the reduction of the weight and volume of such wastes, and also their toxic organic compound content [8,9]. Torrefaction aims is to upgrade the fuel characteristics of biomass such that it can be co-combusted with coal or used as an independent fuel [10]. After torrefaction, biomass is partly decomposed, and produces a solid uniform product with a very low moisture content and a high heating value compared with the raw biomass.

Considering the circular approach, few studies have investigated the char production from several biomasses through a thermal route, and its use as a growth substrate for microalgae [11,12] and leafy vegetables [13]. Even fewer studies haved focused on carbon dioxide biofixation by microalgae, and the potentiality of chars as a growth substrate [14].

A study by Huang et al. (2019) showed the ways in which the co-torrefaction of sewage sludges was adopted for CO_2 removal with an uptake of 53 mg/g [15], even if there are no further developments of the CO_2 fixed. Also in this work, the sewage sludges were considered as low-cost raw materials to produce activated carbons, usable as adsorbents. Thermal treatments are indeed necessary in order to develop the almost non-existent porosity structure of the starting materials, in an attempt to achieve better adsorption capacity performances [16]. In general, the preparation of the precursors is performed through one of the two different routes: physical or chemical activation. Both of the methods foresaw carbonization and an activation phase, accomplished with a one-stage or two-stage process. The carbonization is performed by pyrolyzing the sewage sludges in an inert atmosphere (mainly nitrogen), with a temperature which is often below 800 °C [1,17]. The pyrolysis generates three different products: a volatile and gaseous fraction, vapours and tar components, and solid carbon residue (char) [17,18]. This technique may also be considered as an interesting way to produce valuable fuels: from solid to liquid or syngas phases. Indeed, the operating conditions may be selected to maximize the yield in terms of the desired phase [19]. During the activation process, oxidizing agents like carbon dioxide, air, and steam are adopted in the physical activation process. Meanwhile, activating agents like potassium hydroxide (KOH), sodium hydroxide (NaOH), zinc chloride ($ZnCl_2$), sulfuric acid (H_2SO_4), and phosphoric acid (H_3PO_4), etc. [1] are employed during the chemical activation process. The activation phase is crucial in order to develop a gas cleaning sorbent- like material [2,20–23]. It is necessary to enhance the char structure, increasing, for example, the pore volumes and the specific surface area [24]. In a two-stage process, the first step is related to the char production, while in the second step becomes the crucial activation phase. On the other hand, with a one-stage process, the passage from the carbonization to the activation is performed by switching the flowing gasses (from inert to the oxidizing agent). Starting the thermal process by mixing the feedstock with the activating agent in the chemical scheme can be accomplished. Making a comparison between the two approaches, the one-stage thermal treatment allows us to save time and energy, and increase the final carbon yield [25].

In this study, the physical activation was mainly conducted through thermal activation using an inert gas or an oxidizing gas, such as nitrogen or air and carbon dioxide. During the direct activations, the oxidizing agent was circulated from the beginning of the thermal treatment (transitory and stationary phases).

The goal of this work is to analyse the behaviour of biochar obtained from raw sewage sludges as an adsorbent, to separate the carbon dioxide contained in a typical biogas mixture (CH_4/CO_2 = 1.5). More precisely, the main intention is to investigate the technical feasibility to re-use the anaerobically-digested sewage sludges as activated carbon precursors with the purpose to increase the calorific value of biogas by removing carbon dioxide in a circular economy approach. The final disposal of the CO_2 fixed in the char will be evaluated, considering the char material as a growth substrate for microalgae cultivation, thus increasing the potentiality as a biorefinery case study.

2. Materials and Methods

2.1. Sample Preparation

The anaerobically-digested and dried sewage sludges represent the feedstock for the preparation of the activated carbons. They were produced in the WWTP site of Turin (Castiglione Torinese, Italy). The sludges are characterized by an irregular shape and size, ranging from 1 mm to around 2 cm of equivalent diameter. The chemical composition of the sludges is both a function of the treatments received in the WWTP and the source materials treated in the plant [26]. Table 1 summarizes the feedstock features with three replicates. The biomass was characterized according to ASTM D3172-89 and ASTM D2015, respectively.

Table 1. Characterization of the sewage sludges, as received.

C (%)	35 ± 0.8	As (mg/kg)	5.6 ± 0.28
H (%)	4.8 ± 0.3	Cd (mg/kg)	1.55 ± 0.08
N (%)	4.7 ± 0.1	Cr (mg/kg)	224 ± 5.8
S (%)	<2	Hg (mg/kg)	0.89 ± 0.03
P (%)	2.9 ± 0.08	Ni (mg/kg)	147 ± 1.28
S_{BET} (m^2/g)	0.33 ± 0.016	Pb (mg/kg)	77 ± 3.4
$S_{t\text{-plot ext}}$ (m^2/g)	0.377 ± 0.015	K (mg/kg)	1801 ± 41
$V_{pores\ (d < 1.308\ nm)}$ (cm^3/g)	0.00002 ± $1{\cdot}10^{-6}$	Cu (mg/kg)	388 ± 4.2
$V_{pores\ (d < 44.9\ nm)}$ (cm^3/g)	0.00121 ± $6{\cdot}10^{-5}$	Se (mg/kg)	3.15 ± 0.34
$S_{tot.pores}$ (m^2/g)	0.111 ± $4.3{\cdot}10^{-3}$	Zn (mg/kg)	1109 ± 13

The oxygen percentage may vary approximately in the range of 10–22% [27], while the ashes occupy the remaining percentage. The received sewage sludges were properly milled and sieved before the thermal treatment with a 1 mm size. The reduction in smaller particles was necessary to match the adsorption reactor sizes, and to reduce the diffusion paths during the adsorption tests. It was adopted as an aspect ratio of 15 (the diameter of the reactor/the average particle size).

The sample preparation also required pre- and post-characterization in terms of surface and volume structure. The physical properties of the material were determined using an adsorption-desorption system with nitrogen at 77 K (Micromeritics ASAP 2020 Plus instrument, Norcross, GA, USA). The specific surface area was determined by applying the Brunauer, Emmett and Teller (BET) method to the adsorption data. In this way, the adsorbents are understood and classified for the removal of trace compounds. The volume of the micropores (pores < 2 nm) was calculated using the t-plot method. This method is the most widely used to determine the volume of microporous materials. It is based on standard isothermal data and thickness curves that describe the statistical thickness of the adsorbent film on a sorbent surface. The samples were further characterized in terms of their chemical composition using energy-dispersive X-ray spectroscopy (EDS). The chemical composition can be very useful in order to understand the ways in which surface impregnation affects the adsorption dynamics, the adsorbing interaction with the contaminating molecules, and the adsorption capacity itself.

2.2. Physical Activation and Adsorption Test Equipment

The physical activation of the milled sludges was accomplished in a 57 cm length and 3.4 cm external diameter stainless steel tubular reactor. The sewage sludges loaded inside the reactor were around 150 ± 5 g. The tests were carried out three times. The loaded reactor was placed inside an electric furnace (500 We, C.I.T.T., Messina, Italy), as in the following scheme, see Figure 1. A proportional–integral–derivative (PID) controller managed the electric oven. A temperature regulator model HT MC1 was used to set the heating rate and the residence time of the process (Horst GmbH, Lorsch, Germany). The operating temperature ranged from 200 °C to 600 °C. These values were considered to simulate the coupling with high-temperature fuel cells gas exhausts, see [3,28]. The thermocouple (k-thermocouple, Tersid, Milan, Italy) was placed on the surface of the reactor

inside the oven and connected to the temperature controller. The physical activation was assessed using nitrogen, carbon dioxide and air. Methane and carbon dioxide were used to simulate the biogas mixture in order to examine the carbon dioxide adsorption capacity with the sorbents produced. All of the streams were controlled by a specific mass flow controller (MFC) Bronkhorst (EL-FLOW, AK Ruurlo, Netherland). For temperatures above 300 °C, an oily fraction was formed. This fraction was separated through a glass condenser and kept in a container. Once the thermal activations were accomplished, the activated sewage sludges were adopted for the adsorption tests. In total, 49.5 ± 3.5 g of activated sewage sludges were loaded in a glass reactor. Such filters have an external diameter of 3 cm, while they are filled up to 10 cm height [29]. Cotton gauze was used to support the material loaded into the reactor in order to avoid issues to the mass spectrometer, as reported elsewhere [30,31]. An HPR20QIC mass spectrometer (Hiden Ltd., Warrington, UK) was used to analyse the composition of the gaseous mixture from the output of the reactor. These data were adopted for the generation of the breakthrough curves. The software adopted in combination with the spectrometer was the QGA professional software for Quantitative Gas Analysis (Hiden Ltd., Warrington, UK).

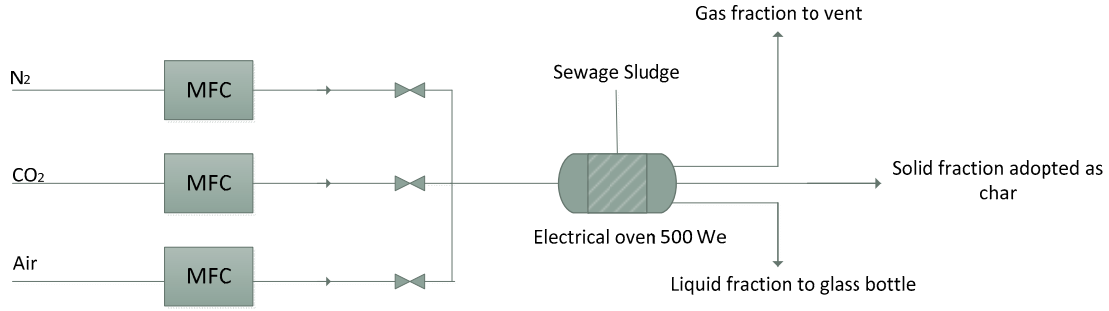

Figure 1. Scheme of the experimental set-up: MFC, mass flow controllers.

3. Results and Discussion

3.1. Char Yield

The sewage sludge thermal treatment is a necessary operation to develop the almost non-existent porosity structure of the starting material (see Table 2). The physical activation was accomplished considering the following parameters:

- Temperature (200–600 °C);
- Residence time (1–2 h);
- Flow rate (300 Nml·min^{-1});
- Heating rate (10 °C·min^{-1});
- Flowing agent (N_2, CO_2, air).

Table 2. Porous structure related to some activated biochar samples. S0, original sample; S1 (400 °C/1 h with CO_2); S2 (400 °C/2 h with CO_2); S23N (400 °C/2 h with N_2); S24N (500 °C/2 h with N_2).

Sample Label	S_{BET} (m^2/g)	$S_{t\text{-Plot ext}}$ (m^2/g)	$V_{pores\ (d < 1.308\ nm)}$ (cm^3/g)	$V_{pores\ (d < 44.9\ nm)}$ (cm^3/g)	$S_{tot.pores}$ (m^2/g)
S0	0.32	0.38	0.00002	0.0012	0.11
S1	2.65	3.27	0.00038	0.0139	2.06
S2	3.29	3.82	0.00024	0.0191	3.48
S23N	2.32	2.75	0.00015	0.0146	2.4
S24N	4.32	4.7	0.00074	0.0226	3.41

The activated char yield is the result of the activation phase to be analysed; Y_{char} is calculated with:

$$Y_{char} = \frac{m_{char}}{m_{raw}} \cdot 100 \quad (1)$$

where m_{char} indicates the mass of the solid quantity remaining in the reactor at the end of the thermal treatment (g), and m_{raw} is the mass of the starting raw material to be activated (g).

The temperature is the parameter that influences the activated char yield value the most. Figure 2 shows how the increase of temperature is followed by a decrease in the activated char yield value, both during the pyrolysis (green lines) and the direct activation with carbon dioxide (blue lines).

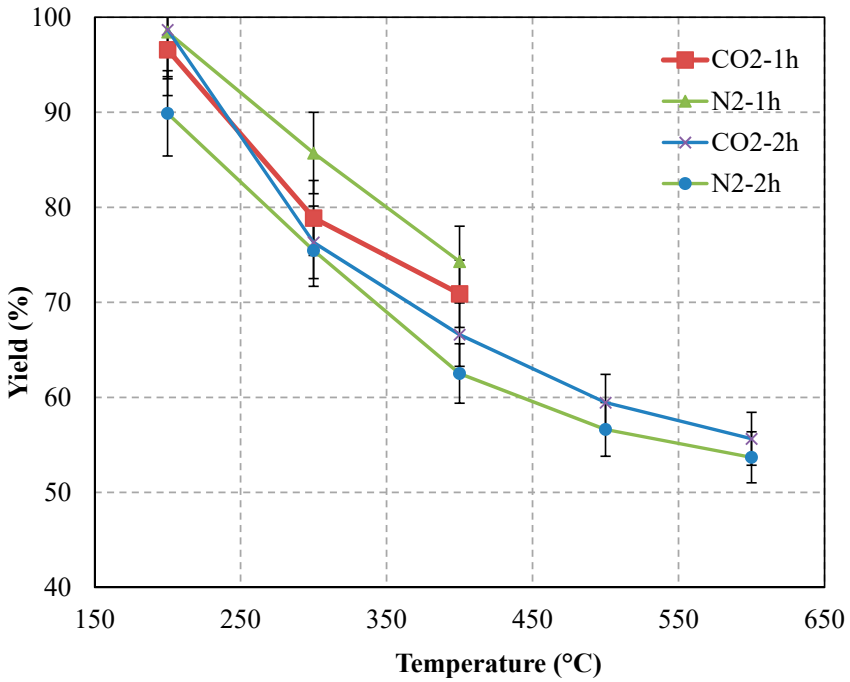

Figure 2. Temperature's influence on the activated char yield during the physical activations.

At a higher residence time (2 h), when coupled with a wider temperature interval (200–600 °C), the reduction of the slope of the curves with the increase of the temperature is more evident. This is caused by the decrease of the volatilization rate. It is possible to recognize different volatilization phases. These are characterized by the emission of substances distinguished with different volatilities. In the low-temperature region, below 300 °C, the weight loss is mainly caused by the volatilization of moisture and some small organic compounds [32]. The considerable difference (around 10%) in the yield of the samples SST2002 hN_2 and SST2002 hCO_2 may be explained by the different moisture content of the raw samples treated in those cases. The initial moisture content increased the yield of char, which affected the pore formation [33].

At temperatures over 300 °C, higher molecular organic compounds start to volatilize and decompose with the formation of an oil fraction [32]. This fraction is mainly composed of tar oil at temperatures above 300 °C. This experiment confirms the literature observations, according to [32,34]. The slope of the graphs is almost constant up to 400 °C, especially with the activations containing nitrogen. This slope indicates a steady volatilization rate. At temperatures of 400–450 °C, the slope of the curves slowly decreased as the temperature increased. This decrease appears to indicate that the most prevalent organic content in the sewage sludges had already decomposed, and that carbonization was taking place. At the highest temperature region, from nearly 450 °C upwards, the yield decreased with a narrower trend. This decrease was caused by the decrease of the organic content. The work of [35] underlines this.

The residence time is the second parameter that affects the activated char yield. One and two hours were the main values analyzed (see Figure 3). A holding time of 3 hours was further considered (at 600 °C) only for the optimization case accomplished for the sample of sewage sludge activated at 600 °C for 2 h in nitrogen (SST6002 hN_2).

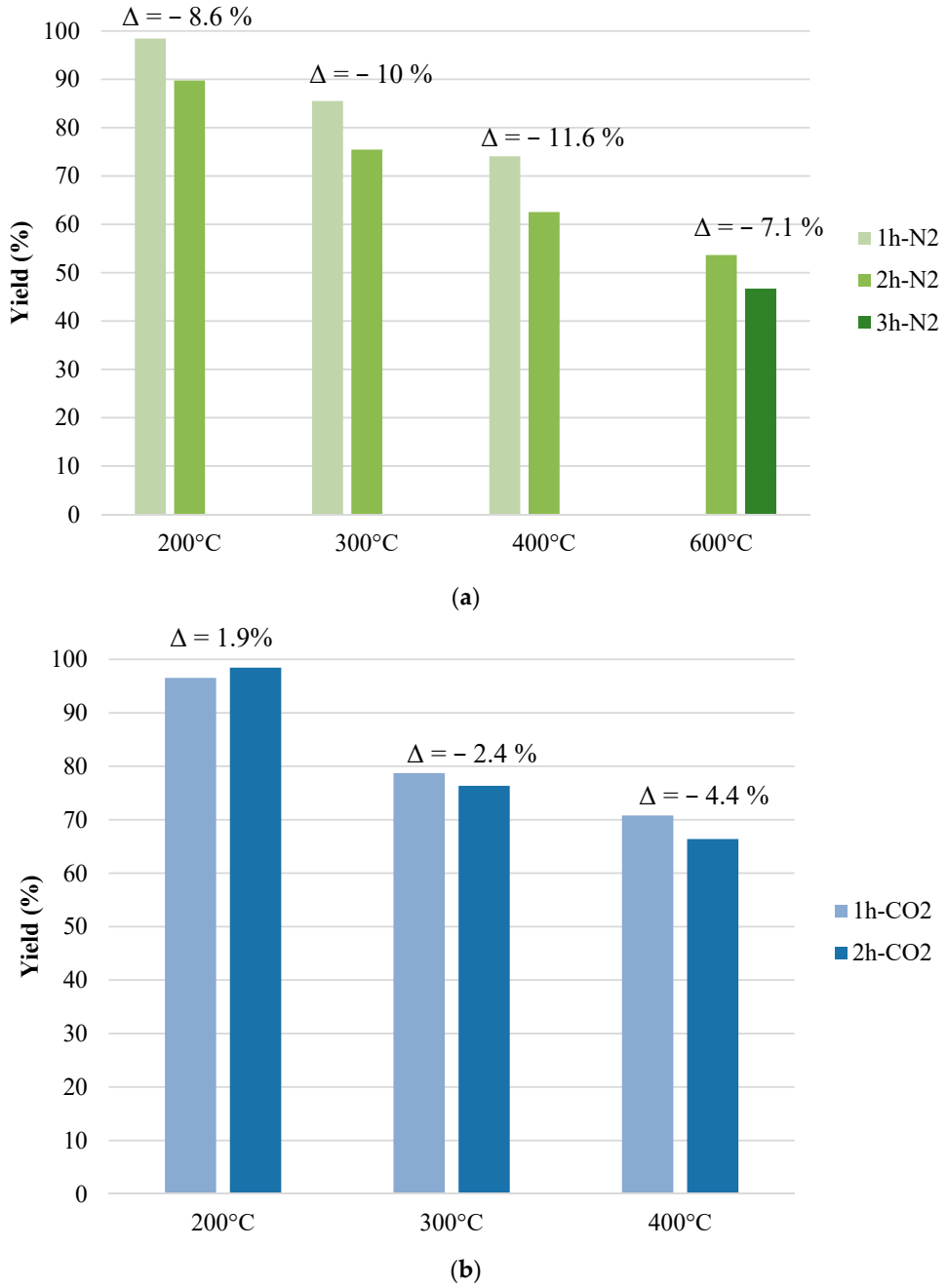

Figure 3. Activated char yield comparison with different residence times, considering as the activating agent: (**a**) N_2, and (**b**) CO_2.

Overall, the activated char yield showed a decrease during the change from one to two hours of residence time (especially for the thermal activations with N_2). Moreover, looking at Figure 3a at 600 °C, the yield value decreased to a smaller extent when the dwell-time was switched from two to three hours. This yield is different from all of the other cases at lower temperatures in the passage from one to two hours. The type of gas employed during the activations (see Figure 4a), the method chosen for the activations (see Figure 4b), the heating rate (see Figure 4c) and the flow rate variation during the activations (a small yield decrease with the flow rate increase, see Figure 4d) did not significantly affect the activated char yield. The most relevant parameters for the activated char yield were therefore clearly demonstrated to be the temperature and the residence time.

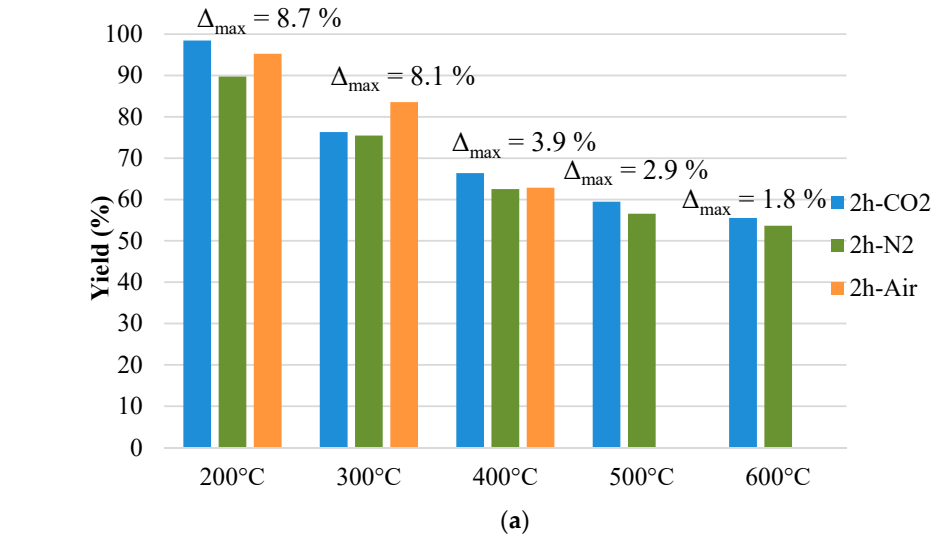

(**a**)

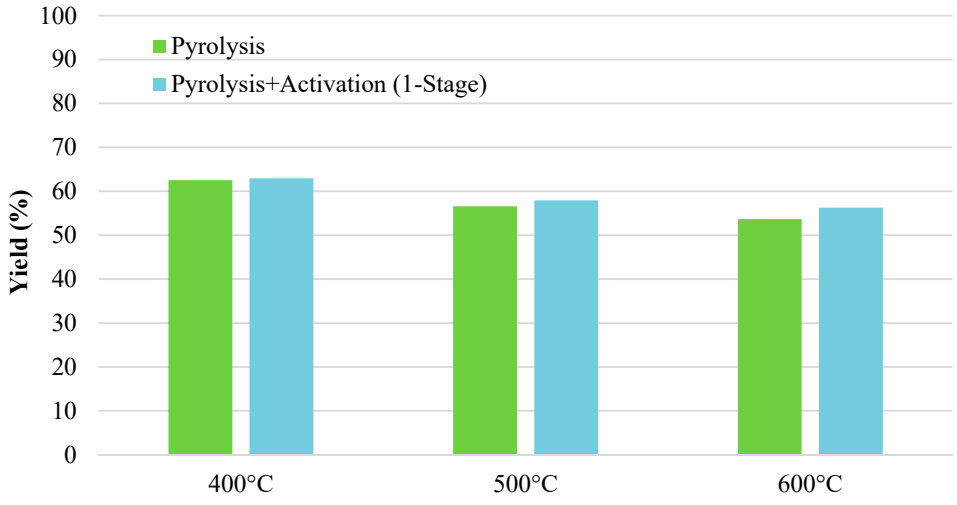

(**b**)

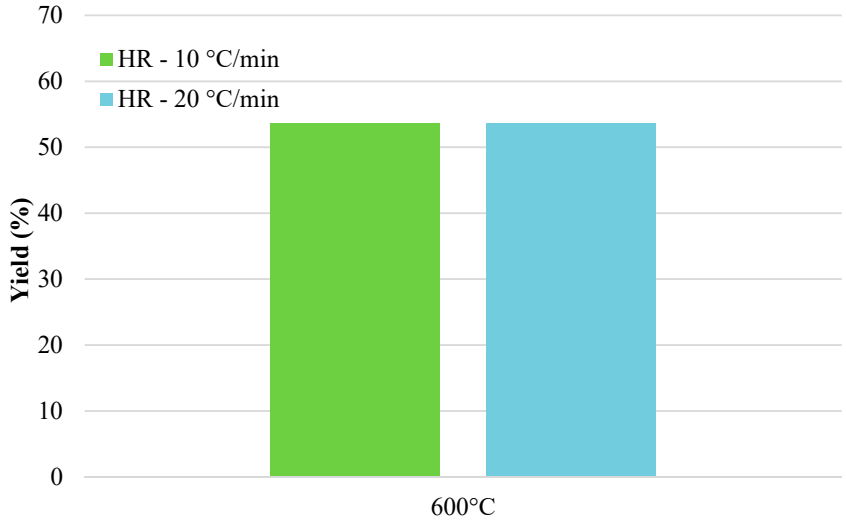

(**c**)

Figure 4. *Cont.*

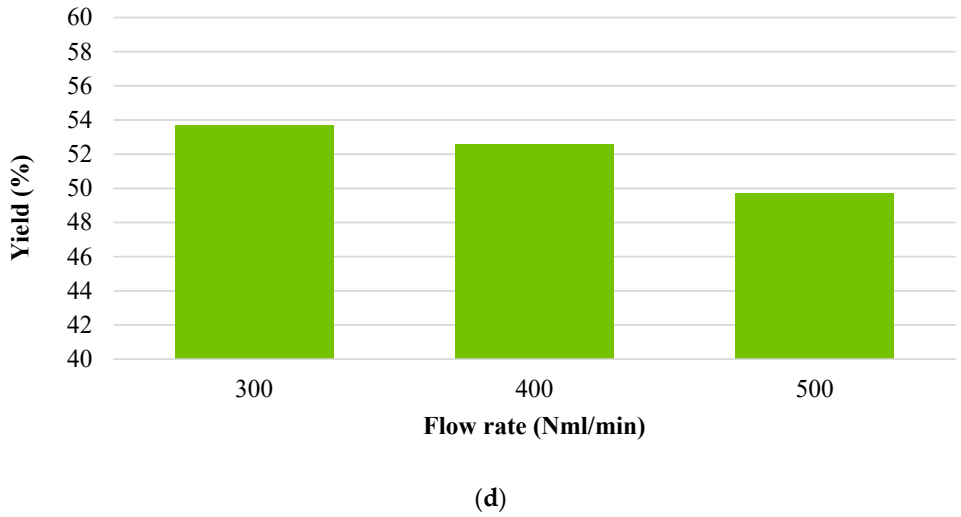

(**d**)

Figure 4. Parameters affecting the char yield: (**a**) activating gas, (**b**) activation method, (**c**) heating rate, and (**d**) flow rate.

3.2. Microscopic Characteristics

The microscopic characteristics of raw and treated sewage sludge were investigated. The surface analysis and chemical compound composition are discussed below. The bar graph in Figure 5 illustrates the percentage concentration variation of selected elements compared to the starting material. The concentration profile depicted agrees with the previous results found in other studies dealing with the thermal treatments of sewage sludges [27,36,37]. The EDS analysis further showed that the most volatile elements detected (C, O) reduced their concentration with the rising temperature. On the contrary, the ash/mineral fraction (Si, Al, Ca, Fe, Mg, K) had an inverse trend in relation to the temperature. The residence time also played an important role. The four samples activated at 400 °C for one hour (with CO_2, and N_2) and two hours (with CO_2, and N_2) showed a conspicuous difference in terms of their concentration variations. The diminution of these elements at the considered temperatures could be explained by the dehydration and decomposition of the organic fraction present in the starting material. The pyrolysis process is widely regarded tas being responsible for the formation of volatile substances like carbon monoxide, carbon dioxide, water and hydrocarbon compounds, through which carbon, oxygen, hydrogen are transported [38]. Nitrogen and hydrogen are other elements that volatilize as a result of the thermal treatment, and thus decrease their concentration [38,39]. The remarkable increase of concentration of the other elements (Si, Al, Ca, Fe, Mg, K) is a consequence of the volatilization of the organic compounds, since the inorganic oxides cannot be volatilized [39]. Moreover, the increase of the mineral fraction as a consequence of the pyrolysis temperature growth determines an increase of the pH level [40]. This increase of the pH level modifies the chemical structure for the surface of the obtained sewage sludge-based biochar. It has been demonstrated that the pyrolysis temperature and the pH are highly correlated ($r^2 = 0.983$, $p < 0.01$) [38]. The r^2 value quantifies this variation, while the *p*-value is less than the significance level (usually 0.05); therefore, such data are well correlated. These aspects affect the char's adsorption capacity.

The activated biochar sample structure slightly improved in comparison to the feedstock material due to physical activation. Table 2 summarizes the results related to the specific areas (the BET and t-Plot methods were adopted) and the volume variation of the selected samples. All of the samples evaluated showed a general improvement in their physical characteristics. However, the activated biochar's textural characteristics revealed a much less developed porosity compared to the commercial activated carbons (generally higher than 1000 m^2/g) [31,41]. These differences may be due to the fact that:

- The high inorganic fraction present in the feedstock which does not volatilize severely limits the porosity development [24];
- The tar fraction produced during the pyrolysis may adhere to the inner activated biochar's surface, and could occlude and block the porous gaps [38];
- The adoption of the physical activation scheme lowers the development of the porosity, rather than the chemical activations [24,27].

The isothermal adsorption/desorption curves of the activated sample at 500 °C for 2 h in nitrogen are shown in the Supplementary Materials (S4). The adsorption isotherm for nitrogen approximates the adsorption curve characteristic of the II Type (according to the IUPAC classification). This category is distinct from the macroporous or nonporous solid adsorbents.

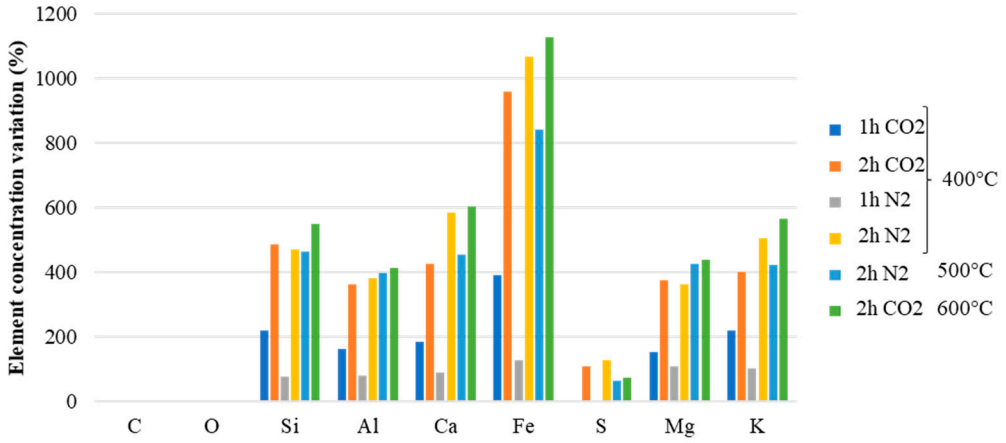

Figure 5. Element concentration variation in comparison with the precursor composition (temperature range 400–600 °C), with N_2 and CO_2 the as activating agents.

3.3. CO_2 Adsorption Capacity

The carbon dioxide capacity was determined by monitoring the response of the fixed-bed column with a simulated biogas blend (35% CO_2 and 65% CH_4) and identifying the breakthrough time from the data recorded by the mass spectrometer. The co-adsorption effects, like acid gasses (e.g., hydrogen sulphide) and siloxanes [42,43] have not been kept into account in the current study. Other relevant parameters for the adsorption tests are the following:

- Biogas flow rate: 153.8 Nml·min^{-1};
- GHSV (gas hourly space velocity): 131·h^{-1};
- C_b: CO_2 breakthrough concentration limit: 2.5%.

The biogas flow rate and the GHSV were not changed during the experimental activity; for this reason, their influence on the adsorption capacity was not examined in the current work. The carbon dioxide adsorption capacity was computed using the following equation:

$$CO_{2cap} = \frac{Q \times t_b \times CO_{2conc} \times 44{,}000}{22.4 \times m_{sorb} \times 10^6} \quad (2)$$

where:

- $CO_{2cap}\left(\frac{mg_{CO_2}}{g_{sorb}}\right)$ is the CO_2 adsorbed in mg per g of sorbent;
- t_b (s) is the breakthrough time;
- $Q\left(\frac{l}{min}\right)$ is the simulated biogas flow rate;
- CO_{2conc} (ppmv) is the total CO_2 concentration in the mixture;

- 44,000 $(\frac{mg}{mol})$ is the CO_2 molar weight;
- 22.4 $\left(\frac{l}{mol}\right)$ is the molar volume of an ideal gas;
- m_{sorb} (g) is the mass of the sorbent;
- 10^6 is the unit conversion from ppmv to molar concentration.

The carbon dioxide breakthrough was fixed to a concentration limit of 2.5%, according to the European limits EN 16723-1 and EN 16723-2 received from the EN 16726. This is the value fixed from the EU Directive for the maximum carbon dioxide concentration allowed in biomethane. These requirements have been adopted for grid injection and its utilization in the transport sector.

The carbon dioxide adsorption capacity was analyzed considering the thermal activation parameters, as performed for the activated char yield in the previous paragraph. All of the results obtained are summarized in Table 3.

Table 3. CO_2 adsorption capacity results.

Sample Label	Adsorption Capacity vwc ($mg_{CO2} \cdot g^{-1}$)	Adsorption Capacity Dry ($mg_{CO2} \cdot g^{-1}$)
S0	4.0	9.9
S11	2.4	4.6
S12	3.7	11.1
S1	4.4	20.1
S21	4.9	6.3
S22	7.7	9.4
S2	16.1	26.2
S23	19.6	49.1
S24	35.0	35.5
S11N	5.2	6.4
S12N	9.9	11.9
S13N	10.6	17.2
S21N	5.1	8.9
S22N	10.9	13.4
S23N	27.7	43.5
S24N	36.5	62.3
S25N	47.7	68.5
SA1	-	5.7
SA2	-	13.0
SA3	-	15.5
SB1	-	18.4
SB2	-	45.7
SB3	-	42.5

S0 original sample, S11 (200 °C/1 h with CO_2), S12 (300 °C/1 h with CO_2), S1 (400 °C/1 h with CO_2), S21 (200 °C/2 h with CO_2), S22 (300 °C/2 h with CO_2), S2 (400 °C/2 h with CO_2), S23 (500 °C/2 h with CO_2), S24 (600 °C/2 h with CO_2), S11N (200 °C/1 h with N_2), S12N (300 °C/1 h with N_2), S13N (400 °C/1 h with N_2), S21N (200 °C/2 h with N_2), S22N (300 °C/2 h with N_2), S23N (400 °C/2 h with N_2), S24N (500 °C/2 h with N_2), S25N (600 °C/2 h with N_2), SA1 (200 °C/2 h with Air), SA2 (300 °C/2 h with Air), SA3 (400 °C/2 h with Air), SB1 (400 °C/2 h with N_2-CO_2), SB2 (500 °C/2 h with N_2-CO_2), SB3 (600 °C/2 h with N_2-CO_2).

The peak temperature achieved during the thermal treatment is one of the most significant parameters in terms of the structural modifications of the feedstock. A positive correlation between the temperature and the carbon dioxide capacity can be observed. The temperature growth is the main factor responsible for the textural changes in the activated biochar sample. The enhancement of the specific surface area and the total pore volume makes more sites available for the carbon dioxide removal. A significant role is also played by the metals' concentrations. The positive correlation between the temperature and the pH makes the activated biochar's structure more neutral/alkaline at the highest range of temperatures, enhancing the number of the "base sites where the carbon dioxide may react like a Lewis acid" [41].

The dwell time is another parameter the value of which influences the filtering performances. For both of the physical activation methods adopted, a higher residence time directly affects the adsorption capacity. This correlation may be due to the release of volatile substances (at the same temperature), which is confirmed by the decrease of the activated char yield value (Figure 3). Table 2 describes the samples obtained with direct carbon dioxide activation at 400 °C (for 1 h and 2 h). A general improvement for physical characteristics was recorded. The BET surface area, the t-plot external surface area, the total volume, and the area were improved, while a slight decrease of the volume with pores smaller than 1.308 nm was recorded.

The outcomes reported above were obtained with variable water content (vwc) in the activated biochar samples. The post activation drying treatments showed better results. Those samples were heated overnight at 100–110 °C and 180 °C, both for pyrolysis and direct carbon dioxide activation. This process was accomplished for the sample that was thermally activated just before the carbon dioxide adsorption test, in order to remove the humidity accumulated from the air. The moisture still contained in the activated samples seemed to have negatively affected the adsorption behaviour of the activated biochar. The water contained in the sorbent structure should be responsible for the reduction of the available pores. Considering the results summarized in Table 3, 400 °C seems to be the minimum carbonization temperature to obtain an acceptable performance.

Considering the activation method's influence, the pyrolysis revealed the best results. The activated biochar samples obtained from the one-stage method and the direct carbon dioxide activation methods had similar behaviours. The direct activation with air was considered only in a low-temperature range (200–400 °C). The air would represent an interesting agent for physical activation due to its costs. Monsalvo et al. obtained similar BET surface areas and micropore volume values in the low range of temperatures (200–400 °C). These values can be comparable to samples activated at much higher temperatures (700–800 °C) [24].

The best-activated biochar sample obtained was the S25N dried (68.5 mg/g), activated at 600 °C in the pyrolysis condition. An optimization was conducted, analysing the effects of the variation of the other parameters on the adsorption performances (residence time, dehydration degree, heating rate, flow rate). The dwell time was the first parameter considered for the optimization process. The reference activated biochar sample (S25N dried) was compared with the same sample activated physically for 3 h (S35N dried). Figure 6a illustrates the ways in which the carbon dioxide adsorption capacity seemed to be almost unchanged when the residence time was switched from 2 to 3 h. Moreover, there aren't significant changes in the activated biochar's structure derived from sewage sludges [24]. The optimal residence time selected was 2 h. This result is advantageous for at least two reasons:

- It gives a higher amount of the solid fraction produced during the physical activation due to the greater yield value (53.7 vs. 46.6%);
- It results in lower energy costs during the thermal treatment for char production.

Further investigations of the post-activation drying treatments were carried out: a temperature of approximately 180 °C was adopted to dry the activated biochar sample S25N overnight after the thermal treatment. In Figure 6b, these performances are shown (S25N dried). This improvement may be due to the greater dehydration degree achieved by the sample treated at the highest temperature. The second parameter that was explored is the flow rate of the nitrogen utilized during the thermal activations, which was fixed at 300 Nml·min^{-1}. In Figure 6c, the S25N dried biochar sample's adsorption capacity is compared with a sample activated and treated in the same conditions, but with a flow rate equal to 500 Nml·min^{-1}. The results showed the sharp decrease of the activated biochar's performances in these conditions. Some authors [44] have reported the trend of the BET surface area and micropore volume with the flow rate variation during the physical activation process. Despite some differences with the current study (the activating agent, the type of feedstock), it has been displayed that below 200 Nml·min^{-1} and above 400 Nml·min^{-1} flow rates, the BET surface area and the micropores volume showed a sudden decrease, identifying a plateau of the optimal values approximately in the flow rate

range values 200–400 Nml·min^{-1}. A similar trend may be hypothesized for the current study too, causing the adsorption capacity of carbon dioxide.

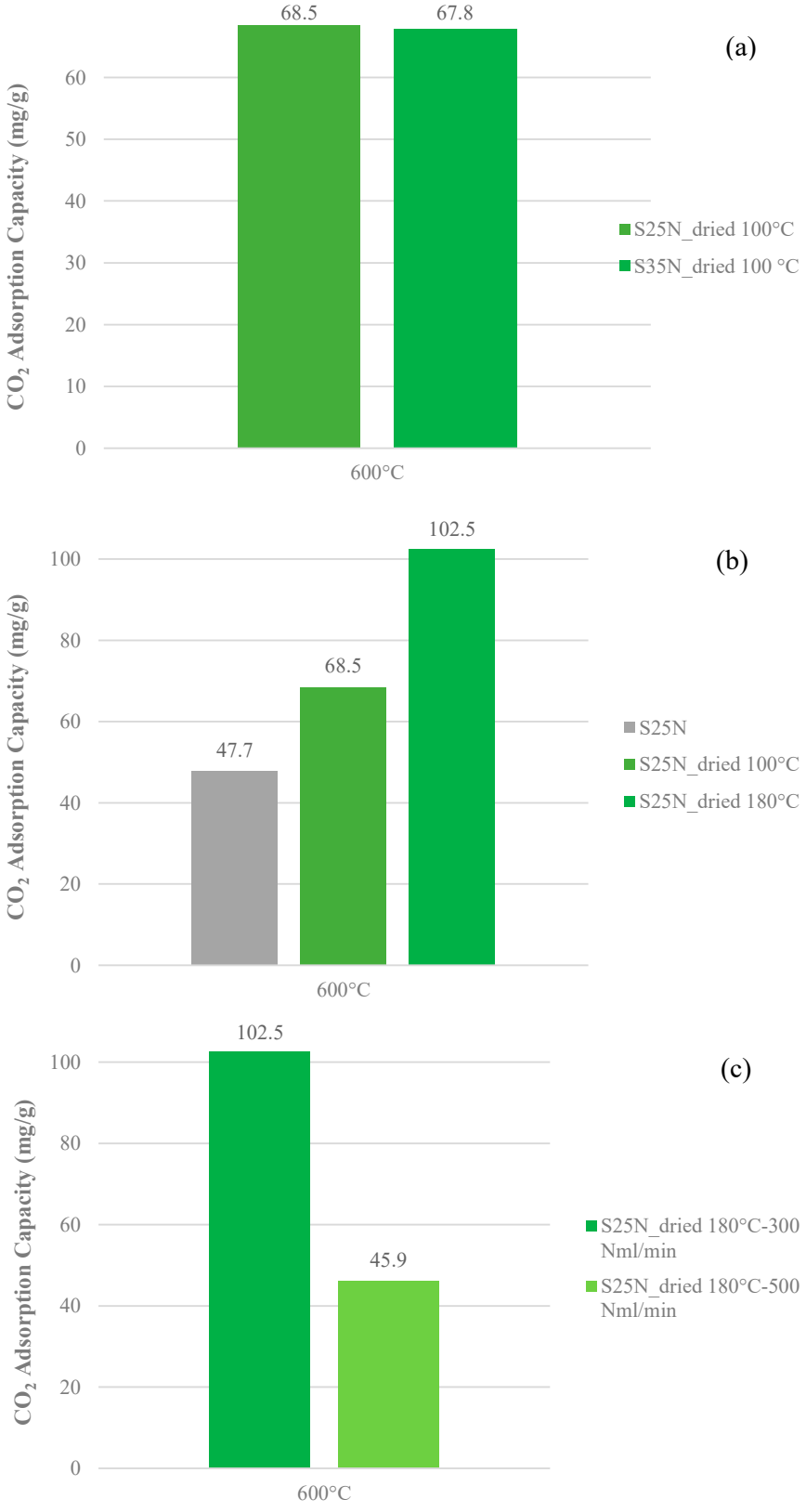

Figure 6. *Cont.*

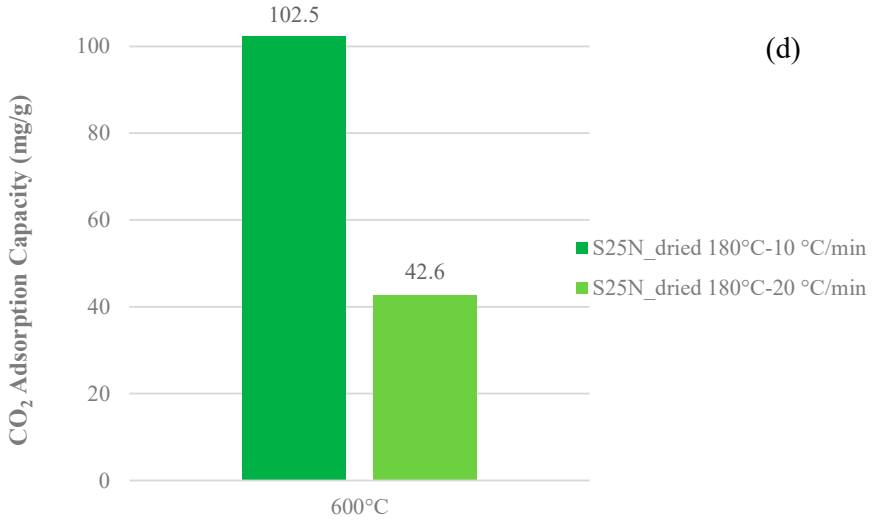

Figure 6. Optimization process influence of: (**a**) the dwell time, (**b**) the post-activation drying temperature, (**c**) the flow rate, and (**d**) the heating rate.

Finally, the last factor considered during the optimization process was the heating rate. Figure 6d shows that the extent to which doubling the eating rate value—from 10 to 20 °C·min^{-1}—affects the adsorption capacity is more than halved in a similar magnitude to what happened for the flow rate increase. The reason may be explained by considering the phenomena ruling the carbonization during the thermal treatments. The transitory phase of the carbonization process is made up by two phases: a softening stage and a shrinkage stage. In the course of the former, a lower heating rate can favour a better formation of the pores, because the gases can be released slowly without the collapse or deformation of the activated char [45]. Moreover, the increase of the heating rate value from 10 to 20 °C·min^{-1} was demonstrated to reduce the BET surface area [45]. Thus, the different porosity development of the two samples may justify the collapse of performances.

At the end of the optimization process, the most efficient sewage sludge-based sorbent for the carbon dioxide separation, with an uptake of 102.5 mg/g, was produced in the following conditions:

- Temperature: 600 °C;
- Dwell time: 2 h;
- Drying temperature: 170–180 °C;
- Physical activation flow rate: 300 Nml·min^{-1};
- Heating rate: 10 °C·min^{-1}.

A similar adsorption capacity result was obtained from other studies considering other starting biomass. Recently, the wood ash from the biomass combustion was adopted for the gas cleaning [46], and there is the possibility to use such ashes for the CO_2 removal for the biomethane production [47]. Juarez et al. (2018) developed a study wherein the fly ash from incinerated waste was adopted for CO_2 removal; the uptake ranged from 35 to 135 kg/t dry ash [46]. Another study, developed by Shimekit et al. (2012), achieved a CO_2 uptake that ranged from 8.8 to 88 mg/g using activated carbons for natural gas purification [48].

Gonzalez et al. (2013) used biomass-based carbon adsorbents for post-combustion CO_2 capture, achieving an uptake that ranged from 66 to 198 mg/g [49].

4. Conclusions

This work stressed the possibility offered by sewage sludges as starting materials for the production of adsorbents. Encouraging results were achieved for carbon dioxide removal. The carbon dioxide removal of such sorbents was also compared to other materials. The thermal activation of sewage

sludges was considered as an effective method for the manufacturing of the carbons. This method follows sequentially the circular economy approach for waste reuse. The pyrolysis of sludges could represent a profitable alternative for the disposal of such waste. Moreover, the production of by-products, such as biofuels, is an interesting consequence to pursue in further research. These fuels can be used for CHP applications (oil and gas) or duty truck engines in the transport sector (oil) [50], etc.

Efforts were dedicated to the optimization of the adsorbents. The most important variables are reported in order of importance: temperature and dwell time. The best adsorption capacity for CO_2 removal (102.5 mg/g) was achieved at an operating temperature of 600 °C, a dwell time of 2 h, and a physical activation flow rate of 300 Nml/min.

Despite these results, a lower temperature was selected (400 °C). This temperature value allows the improvement of energy savings and possible integration with complex systems with high-temperature energy generators, but with limited exhaust temperature gases (400 °C). The results achieved will be used in the industrial scale-up at the WWTP facility in Turin, where a biochar substrate rich with CO_2 will be used for algae production. The preliminary results, already published, will be used for this biomass conversion purpose [51,52].

Supplementary Materials: The following are available online at http://www.mdpi.com/2673-3994/1/1/4/s1, Figure S1: N_2 adsorption/desorption isotherms for the biochar sample SST5002hN2, Figure S2: CO_2 adsorption capacity at different temperature (1–2 h holding time fixed, variable water content), Figure S3: Dwell time comparison between 1 and 2 h for direct activation with CO_2 and pyrolysis (variable water content), Figure S4: Drying treatment effect on the biochar samples activated with a dwell time of 1 h, Figure S5: Drying treatment effect on the biochar samples activated with a dwell time of 2 h, Figure S6: CO_2 adsorption capacity comparison with different methods.

Author Contributions: Conceptualization, D.P., M.S. and M.T.; methodology, D.P. and M.T.; software, D.P. and M.T.; validation, D.P. and M.T.; formal analysis, D.P., M.T. and S.F.; investigation, D.P., M.T. and S.F.; writing—original draft preparation, writing—review and editing, supervision, D.P. and M.S.; project administration, M.S.; funding acquisition, M.S. All authors have read and agreed to the published version of the manuscript.

Funding: This research received no external funding.

Acknowledgments: This paper is a part of the project called "BIOGAS4ENERGY", which is carried out by Politecnico di Torino and other Italian partners (FONDO EUROPEO DI SVILUPPO REGIONALE P.O.R. 2007–2013). A special thanks goes to our technician, Bressan Maurizio.

Conflicts of Interest: The authors declare no conflict of interest.

Nomenclature

BET	Brunauer–Emmett–Teller analytical method
C	carbon content (%)
C_b	CO_2 breakthrough concentration limit
CHP	Combined Heat and Power
CO_{2cap}	CO_2 adsorption capacity ($mg_{CO2} \cdot g_{sorb}^{-1}$)
CO_{2conc}	CO_2 concentration (ppmv)
Dry_x	biochar samples which received further post-drying treatment at the "x" temperature
EDS	Energy Dispersive X-ray Spectrometry
GHSV	Gas Hourly Space Velocity (h^{-1})
H	hydrogen content (%)
IUPAC	International Union of Pure and Applied Chemistry
m_{char}	mass of char (g)
m_{raw}	mass of feedstock (g)
m_{sorb}	mass of sorbent (g)
N	nitrogen content (%)
$N_2/CO_2/Air/N_2$-CO_2	Respectively, nitrogen used only, carbon dioxide used only, air used only, nitrogen for the transitory phase and carbon dioxide for the stationary phase (one-stage method)
P	phosphorous content (%)

PID	proportional–integral–derivative controller
Q	simulated biogas flow rate (l min^{-1})
S	sulfur content (%)
S_{BET}	active surface evaluated with BET method (m^2/g)
SOFC	Solid Oxide Fuel Cell
SS	sewage sludge
$S_{tot.pores}$	total surface of pores (m^2/g)
$S_{t\text{-}plot\ ext}$	active surface evaluated with t-plot method (m^2/g)
t_b	breakthrough time (s)
$V_{pores\ (d < 1.308\ nm)}$	microporous pores (cm^3/g)
$V_{pores\ (d < 44.9\ nm)}$	mesoporous pores (cm^3/g)
vwc	variable water content
WWTP	WasteWater Treatment Plant
y_{char}	Char yield (%)

References

1. Hadi, P.; Xu, M.; Ning, C.; Lin, C.S.K.; McKay, G. A critical review on preparation, characterization and utilization of sludge-derived activated carbons for wastewater treatment. *Chem. Eng. J.* **2015**, *260*, 895–906. [CrossRef]
2. Papurello, D.; Boschetti, A.; Silvestri, S.; Khomenko, I.; Biasioli, F. Real-time monitoring of removal of trace compounds with PTR-MS: Biochar experimental investigation. *Renew. Energy* **2018**, *125*, 344–355. [CrossRef]
3. Santarelli, M.; Briesemeister, L.; Gandiglio, M.; Herrmann, S.; Kuczynski, P.; Kupecki, J.; Lanzini, A.; Llovell, F.; Papurello, D.; Spliethoff, H.; et al. Carbon recovery and re-utilization (CRR) from the exhaust of a solid oxide fuel cell (SOFC): Analysis through a proof-of-concept. *J. CO2 Util.* **2017**, *18*, 206–221. [CrossRef]
4. Sharma, H.B.; Panigrahi, S.; Sarmah, A.K.; Dubey, B. Downstream augmentation of hydrothermal carbonization with anaerobic digestion for integrated biogas and hydrochar production from the organic fraction of municipal solid waste: A circular economy concept. *Sci. Total Environ.* **2020**, *706*, 135907. [CrossRef] [PubMed]
5. Barros, M.V.; Salvador, R.; De Francisco, A.C.; Piekarski, C.M. Mapping of research lines on circular economy practices in agriculture: From waste to energy. *Renew. Sustain. Energy Rev.* **2020**, *131*, 109958. [CrossRef]
6. Kapoor, R.; Ghosh, P.; Kumar, M.; Sengupta, S.; Gupta, A.; Kumar, S.S.; Vijay, V.; Kumar, V.; Vijay, V.K.; Pant, D. Valorization of agricultural waste for biogas based circular economy in India: A research outlook. *Bioresour. Technol.* **2020**, *304*, 123036. [CrossRef]
7. Geissdoerfer, M.; Savaget, P.; Bocken, N.M.; Hultink, E.J. The Circular Economy—A new sustainability paradigm? *J. Clean. Prod.* **2017**, *143*, 757–768. [CrossRef]
8. Samolada, M.; Zabaniotou, A. Comparative assessment of municipal sewage sludge incineration, gasification and pyrolysis for a sustainable sludge-to-energy management in Greece. *Waste Manag.* **2014**, *34*, 411–420. [CrossRef]
9. Prabhakar, A.K.; Mohan, B.C.; Tay, T.S.; Lee, S.S.-C.; Teo, S.L.-M.; Wang, C.-H. Incinerated Sewage Sludge Bottom Ash- Chemical processing, Leaching patterns and Toxicity testing. *J. Hazard. Mater.* **2020**, *402*, 123350. [CrossRef]
10. Gent, S.; Twedt, M.; Gerometta, C.; Almberg, E. *Theoretical and Applied Aspects of Biomass Torrefaction*; Elsevier: Amsterdam, The Netherlands, 2017. [CrossRef]
11. Bolognesi, S.; Bernardi, G.; Callegari, A.; Dondi, D.; Capodaglio, A.G. Biochar production from sewage sludge and microalgae mixtures: Properties, sustainability and possible role in circular economy. *Biomass-Con. Bioref.* **2019**, 1–11. [CrossRef]
12. Shanmugam, S.R.; Adhikari, S.; Nam, H.; Sajib, S.K. Effect of bio-char on methane generation from glucose and aqueous phase of algae liquefaction using mixed anaerobic cultures. *Biomass Bioenergy* **2018**, *108*, 479–486. [CrossRef]
13. Biochar, a potential hydroponic growth substrate, enhances the nutritional status and growth of leafy vegetables -ScienceDirect, (n.d.). Available online: https://www.sciencedirect.com/science/article/pii/S0959652617307886?casa_token=WaP93qJSXUUAAAAA:t4Knu-YZwwoBIuWmoeB2AwS16y3TRDjy-bVxgNqnVZ3Mdr_95Ug0jEzPrkrshQIvOX9tZucoYA (accessed on 18 October 2020).

14. Kassim, M.A.; Meng, T.K. Carbon dioxide (CO2) biofixation by microalgae and its potential for biorefinery and biofuel production. *Sci. Total Environ.* **2017**, *584–585*, 1121–1129. [CrossRef] [PubMed]
15. Huang, Y.-F.; Chiueh, P.-T.; Lo, S.-L. CO2 adsorption on biochar from co-torrefaction of sewage sludge and leucaena wood using microwave heating. *Energy Procedia* **2019**, *158*, 4435–4440. [CrossRef]
16. Florent, M.; Policicchio, A.; Niewiadomski, S.; Bandosz, T.J. Exploring the options for the improvement of H2S adsorption on sludge derived adsorbents: Building the composite with porous carbons. *J. Clean. Prod.* **2020**, *249*, 119412. [CrossRef]
17. Xu, G.; Yang, X.; Spinosa, L. Development of sludge-based adsorbents: Preparation, characterization, utilization and its feasibility assessment. *J. Environ. Manag.* **2015**, *151*, 221–232. [CrossRef]
18. Tang, S.; Tian, S.; Zheng, C.; Zhang, Z. Effect of Calcium Hydroxide on the Pyrolysis Behavior of Sewage Sludge: Reaction Characteristics and Kinetics. *Energy Fuels* **2017**, *31*, 5079–5087. [CrossRef]
19. Trinh, T.N.; Jensen, P.A.; Dam-Johansen, K.; Knudsen, N.O.; Sørensen, H.R. Influence of the Pyrolysis Temperature on Sewage Sludge Product Distribution, Bio-Oil, and Char Properties. *Energy Fuels* **2013**, *27*, 1419–1427. [CrossRef]
20. Shang, G.; Li, Q.; Liu, L.; Chen, P.; Huang, X. Adsorption of hydrogen sulfide by biochars derived from pyrolysis of different agricultural/forestry wastes. *J. Air Waste Manag. Assoc.* **2015**, *66*, 8–16. [CrossRef]
21. Lashaki, M.J.; Fayaz, M.; Wang, H.; Hashisho, Z.; Philips, J.H.; Anderson, J.E.; Nichols, M. Effect of Adsorption and Regeneration Temperature on Irreversible Adsorption of Organic Vapors on Beaded Activated Carbon. *Environ. Sci. Technol.* **2012**, *46*, 4083–4090. [CrossRef]
22. Williams, P.T.; Reed, A. Development of activated carbon pore structure via physical and chemical activation of biomass fibre waste. *Biomass Bioenergy* **2006**, *30*, 144–152. [CrossRef]
23. Papurello, D.; Tomasi, L.; Silvestri, S.; Belcari, I.; Santarelli, M.; Smeacetto, F.; Biasioli, F. Biogas trace compound removal with ashes using proton transfer reaction time-of-flight mass spectrometry as innovative detection tool. *Fuel Process. Technol.* **2016**, *145*, 62–75. [CrossRef]
24. Monsalvo, V.M.; Mohedano, A.F.; Rodríguez, J.J. Activated carbons from sewage sludge. *Desalination* **2011**, *277*, 377–382. [CrossRef]
25. Girgis, B.S.; Khalil, L.B.; Tawfik, T.A. Porosity Development in Carbons Derived from Olive Oil Mill Residue Under Steam Pyrolysis. *J. Porous Mater.* **2002**, *9*, 105–113. [CrossRef]
26. Smith, K.; Fowler, G.; Pullket, S.; Graham, N. Sewage sludge-based adsorbents: A review of their production, properties and use in water treatment applications. *Water Res.* **2009**, *43*, 2569–2594. [CrossRef]
27. Ros, A.; Lillo-Ródenas, M.; Fuente, E.; Montes-Morán, M.; Martín, M.; Linares-Solano, A. High surface area materials prepared from sewage sludge-based precursors. *Chemosphere* **2006**, *65*, 132–140. [CrossRef]
28. Papurello, D.; Silvestri, S.; Lanzini, A. Biogas cleaning: Trace compounds removal with model validation. *Sep. Purif. Technol.* **2019**, *210*, 80–92. [CrossRef]
29. Gabelman, A. Adsorption Basics: Part 1. *Chem. Eng. Prog.* **2017**, *113*, 48–53.
30. Papurello, D.; Tomasi, L.; Silvestri, S. Proton transfer reaction mass spectrometry for the gas cleaning using commercial and waste-derived materials: Focus on the siloxane removal for SOFC applications. *Int. J. Mass Spectrom.* **2018**, *430*, 69–79. [CrossRef]
31. Papurello, D.; Tomasi, L.; Silvestri, S.; Santarelli, M. Evaluation of the Wheeler-Jonas parameters for biogas trace compounds removal with activated carbons. *Fuel Process. Technol.* **2016**, *152*, 93–101. [CrossRef]
32. Cheng, F.; Luo, H.; Hu, L.; Yu, B.; Luo, Z.; De Cortalezzi, M.F. Sludge carbonization and activation: From hazardous waste to functional materials for water treatment. *J. Environ. Chem. Eng.* **2016**, *4*, 4574–4586. [CrossRef]
33. Demirbas, A. Effects of temperature and particle size on bio-char yield from pyrolysis of agricultural residues. *J. Anal. Appl. Pyrolysis* **2004**, *72*, 243–248. [CrossRef]
34. Cao, Y.; Pawłowski, A. Sewage sludge-to-energy approaches based on anaerobic digestion and pyrolysis: Brief overview and energy efficiency assessment. *Renew. Sustain. Energy Rev.* **2012**, *16*, 1657–1665. [CrossRef]
35. Linghu, W.; Shen, R. Thermal behaviour of sewage sludge in pyrolysis process. *Mater. Res. Innov.* **2014**, *18*, S4–S50. [CrossRef]
36. Ortiz, F.G.; Aguilera, P.; Ollero, P. Biogas desulfurization by adsorption on thermally treated sewage-sludge. *Sep. Purif. Technol.* **2014**, *123*, 200–213. [CrossRef]

37. Hossain, M.K.; Strezov, V.; Chan, K.Y.; Ziolkowski, A.; Nelson, P.F. Influence of pyrolysis temperature on production and nutrient properties of wastewater sludge biochar. *J. Environ. Manag.* **2011**, *92*, 223–228. [CrossRef] [PubMed]
38. Jin, J.; Li, Y.; Zhang, J.; Wu, S.; Cao, Y.; Liang, P.; Zhang, J.; Wong, M.H.; Wang, M.; Shan, S.; et al. Influence of pyrolysis temperature on properties and environmental safety of heavy metals in biochars derived from municipal sewage sludge. *J. Hazard. Mater.* **2016**, *320*, 417–426. [CrossRef] [PubMed]
39. Magdziarz, A.; Werle, S. Analysis of the combustion and pyrolysis of dried sewage sludge by TGA and MS. *Waste Manag.* **2014**, *34*, 174–179. [CrossRef] [PubMed]
40. Zielińska, A.; Oleszczuk, P.; Charmas, B.; Skubiszewska-Zięba, J.; Pasieczna-Patkowska, S. Effect of sewage sludge properties on the biochar characteristic. *J. Anal. Appl. Pyrolysis* **2015**, *112*, 201–213. [CrossRef]
41. De Andrés, J.M.; Orjales, L.; Narros, A.; Fuente, M.D.M.D.L.; Rodríguez, M.E. Carbon dioxide adsorption in chemically activated carbon from sewage sludge. *J. Air Waste Manag. Assoc.* **2013**, *63*, 557–564. [CrossRef]
42. Papurello, D.; Gandiglio, M.; Kafashan, J.; Lanzini, A. Biogas Purification: A Comparison of Adsorption Performance in D4 Siloxane Removal Between Commercial Activated Carbons and Waste Wood-Derived Char Using Isotherm Equations. *Processes* **2019**, *7*, 774. [CrossRef]
43. Cabrera-Codony, A.; Santos-Clotas, E.; Ania, C.O.; Martín, M.J. Competitive siloxane adsorption in multicomponent gas streams for biogas upgrading. *Chem. Eng. J.* **2018**, *344*, 565–573. [CrossRef]
44. Yang, K.; Peng, J.; Xia, H.; Zhang, L.; Srinivasakannan, C.; Guo, S. Textural characteristics of activated carbon by single step CO2 activation from coconut shells. *J. Taiwan Inst. Chem. Eng.* **2010**, *41*, 367–372. [CrossRef]
45. Tay, J.; Chen, X.; Jeyaseelan, S.; Graham, N. Optimising the preparation of activated carbon from digested sewage sludge and coconut husk. *Chemosphere* **2001**, *44*, 45–51. [CrossRef]
46. Juárez, M.F.-D.; Mostbauer, P.; Knapp, A.; Müller, W.; Tertsch, S.; Bockreis, A.; Insam, H. Biogas purification with biomass ash. *Waste Manag.* **2018**, *71*, 224–232. [CrossRef]
47. Lombardi, L.; Costa, G.; Spagnuolo, R. Accelerated carbonation of wood combustion ash for CO2 removal from gaseous streams and storage in solid form. *Environ. Sci. Pollut. Res.* **2018**, *25*, 35855–35865. [CrossRef]
48. Javadzadeh, Y.; Hamedeyazdan, Y.J.A.S. Floating Drug Delivery Systems for Eradication of Helicobacter pylori in Treatment of Peptic Ulcer Disease. *Trends in Helicobacter pylori Infection* **2014**, *i*, 13. [CrossRef]
49. González, A.; Plaza, M.; Rubiera, F.; Pevida, C. Sustainable biomass-based carbon adsorbents for post-combustion CO2 capture. *Chem. Eng. J.* **2013**, *230*, 456–465. [CrossRef]
50. Hornung, A.; Neumann, J.; Daschner, R. *Sustainable Utilization Of Municipal, (n.d.)*; IWWG: Padua, Italy, 2018; pp. 21–23.
51. Papurello, D.; Bressan, M.; Bona, D.; Flaim, G.; Cerasino, L.; Silvestri, S. Simulated Sofc Exhausts and Their Fixation on Chlorella Vulgaris: Study on Affecting Parameters. *Detritus* **2019**, *5*, 99–104. [CrossRef]
52. Bona, D.; Papurello, D.; Flaim, G.; Cerasino, L.; Biasioli, F.; Silvestri, S. Management of Digestate and Exhausts from Solid Oxide Fuel Cells Produced in the Dry Anaerobic Digestion Pilot Plant: Microalgae Cultivation Approach. *Waste Biomass-Valorization* **2020**, 1–16. [CrossRef]